ISSN: 2181-3337 | SCIENTISTS.UZ VOLUME 5 ISSUE 8 AUGUST 2026

MAXWELL–WAGNER OBSERVABILITY ANALYSIS IN TWO-FREQUENCY CAPACITIVE MEASUREMENT OF WATER CONTENT AND DENSITY IN HYDROCARBON EMULSIONS

Eshmuradov Dilshod[1], **Ismailov Otabek**[2], **Nizomov Norkhuja**[3]
Tashkent University of Information Technologies
named after Muhammad al-Khwarizmi, Tashkent, Uzbekistan[1,2,3]

DOI: 10.67620/sai.58a0003

ABSTRACT

Capacitive transducers are widely used for in-line control of fuels and other hydrocarbon media, but a single-frequency reading of effective permittivity cannot separate the water content of an emulsion from the density of the hydrocarbon phase because both quantities shift the same scalar output. This study formulates the separation task as a parameter-observability problem and shows that Maxwell–Wagner interfacial polarization provides the physical mechanism required to resolve it. A Maxwell–Garnett mixture model with complex phase permittivities was combined with the Clausius–Mossotti relation linking hydrocarbon density to permittivity, and the Jacobian of the two-frequency measurement map was analysed over a five-decade band. The determinant of the Jacobian vanishes identically when the two probing frequencies coincide, demonstrating that a second frequency is a necessary condition for observability rather than merely an accuracy refinement. Numerical analysis places the practical optimum at a low frequency below 0.05 of the relaxation frequency and a high frequency above ten times it; beyond this separation, the gain saturates within 1%. With a channel resolution of $1 \cdot 10^{-4}$ in relative permittivity, the propagated standard uncertainties are 0.033% for water volume fraction and 1.07 kg/m³ for density; Monte Carlo inversion reproduced these values and revealed negligible bias. The scheme was tolerant to salinity: a 50% error in the assumed water conductivity displaced the density estimate by only 0.11 kg/m³.

ACCEPTED

03.09.26

Keywords: *Maxwell–Wagner polarization; capacitive transducer; water content; observability; measurement uncertainty.*

CC BY

Introduction

In-line quality control of liquid hydrocarbons requires two quantities to be known simultaneously: the water content of the medium and the density of the hydrocarbon phase. The first governs the commercial and operational acceptability of the product; the second provides information on composition and on the presence of lighter or heavier fractions. Capacitive transducers are attractive for this task because they are non-intrusive, inexpensive, and directly sensitive to the dielectric properties of the medium (Sihvola, 1999).

The difficulty is structural rather than technological. A capacitive cell filled with a water-in-oil emulsion returns a single scalar: the effective relative permittivity of the mixture. Water raises this value because the permittivity of water exceeds that of a hydrocarbon by nearly two orders of magnitude; density

raises it as well because a denser hydrocarbon is more polarizable per unit volume. Two independent causes therefore act on one observable, and no improvement in the electronics can remove that ambiguity. The problem is one of observability in the sense used in system theory (Kalman, 1963): the map from parameters to measurements must be locally invertible before any estimation procedure can be meaningful.

Interfacial polarization offers a way out. When a heterogeneous medium contains phases with different conductivities, charge accumulates at internal interfaces and produces dielectric dispersion with a characteristic relaxation frequency. The effect was described by Maxwell (1873), given a dispersive formulation by Wagner (1914), extended to non-spherical inclusions by Sillars (1937), and extended to concentrated systems by Hanai (1960). Its central feature for the present purpose is that the dispersion is governed by the conductivity and volume fraction of the dispersed phase, whereas the permittivity of the continuous phase enters the response in a different functional form. The frequency axis therefore carries information that a single reading discards.

Interfacial polarization in emulsions and composites remains an active field. Asami (2002) surveyed the theory for two-, three-, and multiphase systems; Adohi et al. (2009) applied the Maxwell–Wagner–Hanai effective-medium description to conducting composite films; Samet et al. (2022) established scaling laws relating the characteristic frequency to the conductivity of the dispersed phase; and Qian et al. (2022) proposed an integral modification of the Maxwell–Wagner model for emulsions at higher volume fractions. These works establish the forward problem, that is, the prediction of permittivity from composition. The inverse problem relevant to measurement practice—whether and under what conditions composition can be recovered from permittivity readings—has received much less attention. In parallel, the metrological aspects of related measurement tasks have been addressed; for example, radio-transparency measurements of composite (i.e., structurally heterogeneous) materials have been placed on a metrological basis (Jumamuratov et al., 2024). Those studies, however, address the forward measurement task and do not consider the recovery of several composition parameters from one channel.

This paper addresses that gap. The aim is not to propose another mixture formula but to establish, for a two-frequency capacitive channel, the condition under which water content and hydrocarbon density become separable and to convert that condition into engineering requirements: which frequencies to choose and what resolution the measurement channel must achieve. Three questions are addressed. First, is a second frequency merely helpful or strictly necessary? Second, where should the two frequencies be placed relative to the relaxation frequency? Third, what uncertainty in the recovered quantities follows from a given uncertainty in the permittivity reading?

Methods

Dielectric model of the medium

The medium is treated as a water-in-oil emulsion of spherical droplets dispersed in a continuous hydrocarbon phase. For volume fractions below about 0.15, the Maxwell–Garnett mixing rule with complex phase permittivities describes the effective response adequately (Asami, 2002; Sihvola, 1999):

$$\varepsilon_{mix}^{*} = \varepsilon_{h}^{*}\frac{2\varepsilon_{h}^{*}+\varepsilon_{i}^{*}+2\varphi\left(\varepsilon_{i}^{*}-\varepsilon_{h}^{*}\right)}{2\varepsilon_{h}^{*}+\varepsilon_{i}^{*}\left(\varepsilon_{i}^{*}-\varepsilon_{h}^{*}\right)} \quad (1)$$

where φ is the volume fraction of the dispersed phase, and the complex permittivity of each phase is written as

$$\varepsilon^{*} = \varepsilon - j\frac{\sigma}{\omega\varepsilon_{0}} \quad (2)$$

where σ is the conductivity, ω is the angular frequency, and ε_0 is the electric constant. Subscript h denotes the host hydrocarbon, and subscript i denotes the water inclusions.

The link between the density of the hydrocarbon phase and its permittivity is supplied by the Clausius–Mossotti relation, which, for a given hydrocarbon class, uses a constant specific refraction, A (Böttcher, 1973):

ISSN: 2181-3337 | SCIENTISTS.UZ

$$\frac{\varepsilon_h - 1}{\varepsilon_h + 2} = A\rho, \quad \varepsilon_h = \frac{1 + 2A\rho}{1 - 2A\rho} \tag{3}$$

Calibrating A at the reference point $\rho = 840\,kg/m^3$ and $\varepsilon_h = 2.10$ gives $A = 3.194 \cdot 10^{-4}\,m^3/kg$, which maps the density interval $800 - 880\,kg/m^3$ to the permittivity interval 2.030–2.173. This narrow interval is the origin of the conditioning problem examined below.

In the dilute limit, the interfacial-polarization relaxation frequency follows from the conductivity of the dispersed phase and the permittivities of both phases:

$$f_{\mathrm{MW}} = \frac{\sigma_i}{2\pi\varepsilon_0(\varepsilon_i + 2\varepsilon_h)} \tag{4}$$

Formulation of the observability problem

Let the parameter vector be $\mathrm{x} = (\varphi, \rho)$ and the measurement vector $y = \left(\varepsilon'(f_1), \varepsilon'(f_2)\right)$, where ε' denotes the real part of the effective permittivity. Only the real part is used because a capacitance reading is the quantity delivered directly by a charge-transfer front end. The measurement map is $y = h(x)$, and local observability requires the Jacobian

$$J = \frac{\partial\left(\varepsilon'(f_1), \varepsilon'(f_2)\right)}{\partial(\varphi, \rho)} \tag{5}$$

to be non-singular at the operating point. If $f_1 = f_2$, the two rows of J are identical and $detJ = 0$ for every x. Therefore, the parameters cannot be separated at any single frequency, irrespective of measurement quality. This is the formal statement of the necessity of a second frequency. The magnitude of $\det J$ then measures how far the configuration is from that degenerate case, whereas the condition number of J governs how measurement noise is amplified in the estimates.

Uncertainty is propagated in accordance with the Guide to the Expression of Uncertainty in Measurement (Joint Committee for Guides in Metrology [JCGM], 2008). For uncorrelated readings of equal standard uncertainty $u\varepsilon'$, the standard uncertainties of the estimated parameters follow from the rows of the inverse Jacobian:

$$u(\mathrm{x_k}) = u(\varepsilon')\sqrt{(J^{-1})_{k1}^2 + (J^{-1})_{k2}^2} \tag{6}$$

Uncertainty alone, however, does not exhaust the metrological description of an adaptive channel: the interval over which the stated uncertainty remains valid is itself an object of analysis, and criteria of metrological reliability are required to justify that interval (Sharipov et al., 2022).

Measurement scheme

Figure 1 shows the arrangement assumed throughout. A coaxial measuring cell is excited alternately at the two frequencies; a charge-transfer front end converts the cell capacitance into a code; a reference capacitor outside the cell supports periodic autocalibration of the conversion scale; and an inversion unit recovers the pair (φ, ρ) from the two permittivity readings. The inversion is performed using Newton iteration on the residuals of Equations (1)–(3), with the Jacobian evaluated by central differences at each step.

ISSN: 2181-3337 | SCIENTISTS.UZ

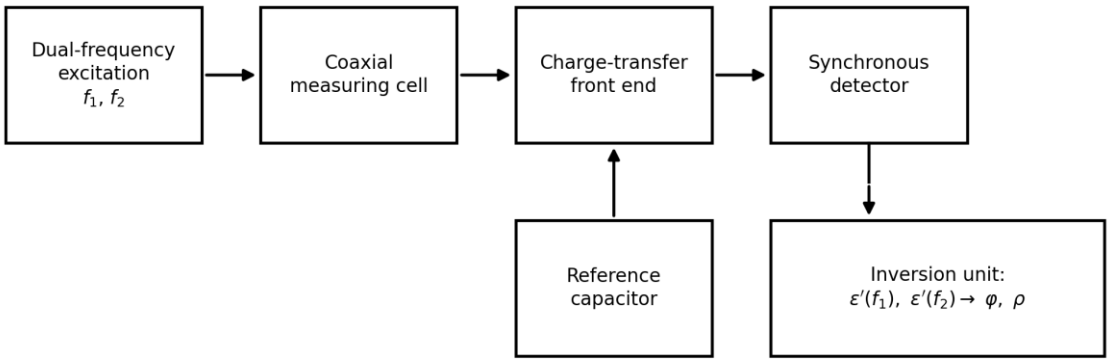


Figure 1. Functional diagram of the two-frequency capacitive measurement channel

Numerical experiment

The phase parameters used in the computations are listed in Table 1. The adopted water relative permittivity is consistent with dielectric-property data reported by Kaatze (1989). The water conductivity corresponds to weakly mineralized water, which places the relaxation frequency in the megahertz region and therefore within reach of a practical capacitive front end.

Table 1. *Parameters of the phases adopted in the computations*

Quantity	**Symbol**	**Value**	**Unit**
Water relative permittivity	εi	80.1	—
Water conductivity	σi	$1 \cdot 10^{-2}$	S/m
Hydrocarbon conductivity	σh	$1 \cdot 10^{-10}$	S/m
Specific refraction	A	$3.194 \cdot 10^{-4}$	m³/kg
Density range	ρ	800 … 880	kg/m³
Water volume fraction range	φ	0.005 … 0.12	—
Operating point	φ_0, ρ_0	0.05; 840	—; kg/m³
Relaxation frequency at ρ_0	[redacted]	$2.13 \cdot 10^6$	Hz

Four computations were carried out. The dispersion curve $\varepsilon'(f)$ was evaluated over six decades for several water fractions. The determinant of the Jacobian was mapped over a grid of frequency pairs spanning five decades. Propagated uncertainties were computed from equation (6) for selected frequency pairs and for a range of channel resolutions. Finally, a Monte Carlo experiment with 500 realizations per operating point verified the propagated values and tested the inversion for bias.

Results

Dielectric dispersion of the medium

Figure 2 shows the computed dispersion. Below the relaxation frequency the water droplets behave as conducting inclusions and the effective permittivity approaches the limit $\varepsilon_h\,(1 + 2\varphi)/(1 - \varphi)$; above it the droplets act as high-permittivity dielectric inclusions and the mixture value falls. For φ = 0.05 the total dispersion depth is 0.026 units of relative permittivity, that is 1.1% of the level, and the transition is centred at 2.13 MHz. The dispersion depth grows with water content, which is precisely the behaviour that makes the frequency axis informative.

ISSN: 2181-3337 | SCIENTISTS.UZ

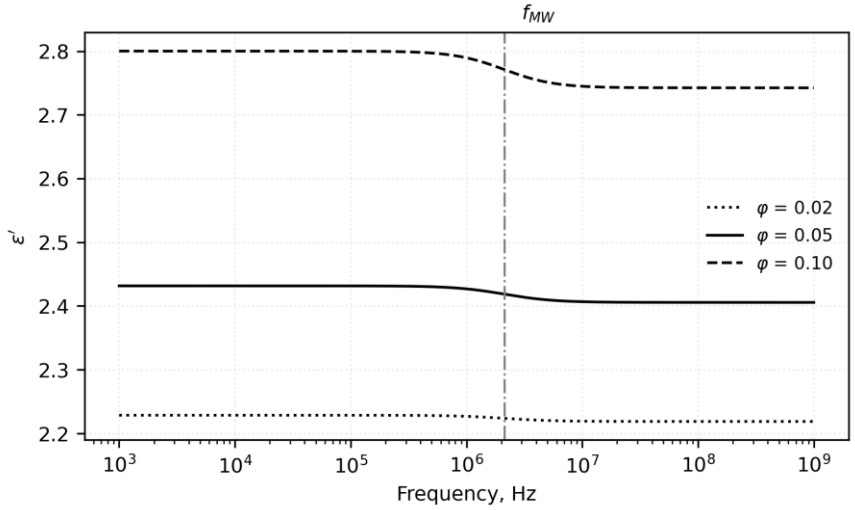


Figure 2. Effective permittivity against frequency for three water volume fractions at $\rho = 840\,kg/m^3$

Single-frequency ambiguity

The ambiguity anticipated on theoretical grounds is complete rather than partial. At 1 MHz the value $\varepsilon' = 2.42686$ is reproduced exactly by every pair listed in Table 2, which traces a continuous locus across the whole plausible range of both parameters. A single-frequency instrument cannot distinguish 2% water in a heavy hydrocarbon from 9% water in a light hydrocarbon.

Table 2. *Parameter pairs producing an identical permittivity reading at 1 MHz*

Water volume fraction φ, %	2.0	3.0	4.0	5.0	6.0	7.0	8.0	9.0
Density $\rho, kg/m^3$	940.9	907.0	873.4	840.0	806.8	773.8	741.0	708.4

Figure 3 shows the same result geometrically. Each frequency defines a locus of constant reading in the (φ, ρ) parameter plane; two frequencies define two loci whose intersection is the solution. The loci intersect at a single point, confirming observability, but they cross at a small angle. That small angle is the geometric expression of the ill-conditioning quantified below.

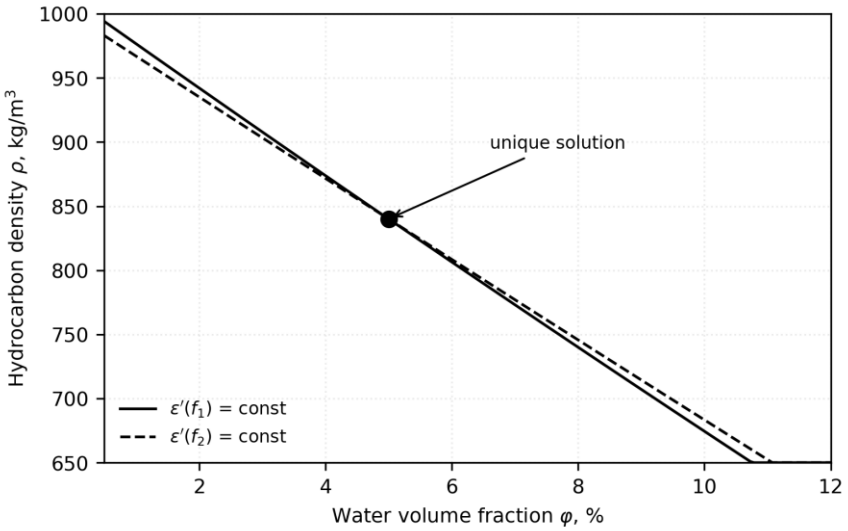


Figure 3. Loci of constant permittivity at the two probing frequencies in the parameter plane

Observability map

Figure 4 maps the determinant of the Jacobian over the plane of frequency pairs. The diagonal $f_1 = f_2$ appears as a line of exact singularity, in agreement with the analytical argument. Observability rises monotonically as the pair straddles the relaxation frequency and reaches its maximum when one frequency

ISSN: 2181-3337 | SCIENTISTS.UZ

lies far below f_{MW} and the other far above it. Over the grid examined, the maximum determinant was $8.85 \cdot 10^{-4}$, attained at $f_1 = 1.5 \cdot 10^{-3} f_{\mathrm{MW}}$ and $f_2 = 148 f_{\mathrm{MW}}$, with a condition number of $1.02 \cdot 10^{5}$.

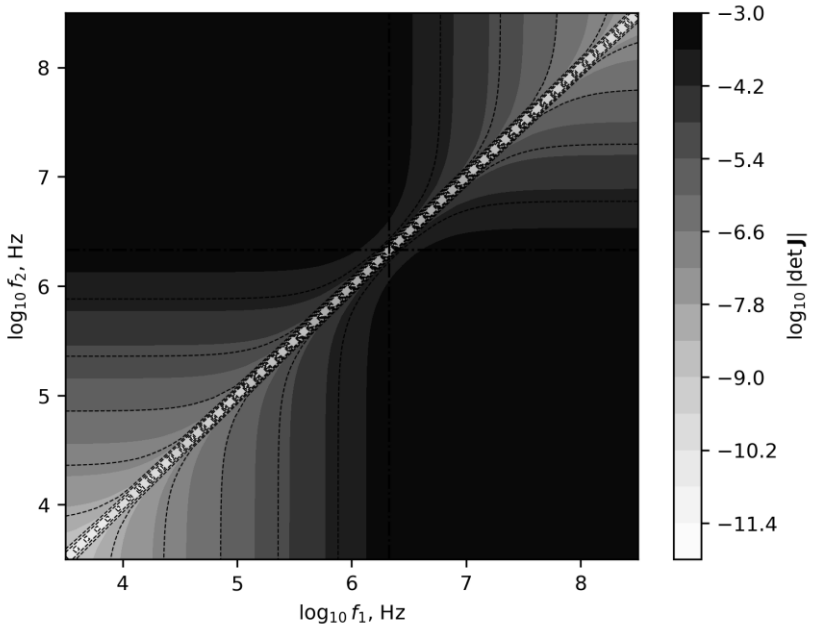


Figure 4. Decimal logarithm of the Jacobian determinant against the two probing frequencies; dash-dotted lines mark f_{MW}

The practical consequence is milder than the location of the formal optimum suggests. Table 3 lists the propagated uncertainties for frequency pairs expressed as multiples of f_{MW}. Once the low frequency is at or below $0.05 f_{\mathrm{MW}}$ and the high frequency at or above $10 f_{\mathrm{MW}}$, further separation improves the result by less than 1%. This yields a simple design rule that does not demand extreme frequencies.

Table 3. *Propagated standard uncertainties for frequency pairs referred to the relaxation frequency, at* $u(\varepsilon') = 1 \cdot 10^{-4}$

f_1	f_2	u(φ), %	u(ρ), kg/m³
0.500·	2·	0.0546	1.784
0.500·		0.0414	1.344
0.500·	50·	0.0409	1.327
0.050·	2·	0.0412	1.354
0.050·		0.0332	1.085
0.050·	50·	0.0329	1.074
0.005·		0.0331	1.082
0.005·	50·	0.0328	1.071

Required resolution of the measuring channel

Because the density interval maps onto a narrow permittivity interval, the conditioning of the problem translates directly into a requirement on the channel. Table 4 gives the propagated uncertainties for the pair 10 kHz and 100 MHz as a function of the resolution in relative permittivity. A resolution of $2 \cdot 10^{-3}$, typical of an uncompensated capacitive channel, would render the density estimate impractical. A resolution of $1 \cdot 10^{-4}$, which corresponds to roughly 40 parts per million of the measured capacitance, reduces the density uncertainty to about 1 kg/m³.

ISSN: 2181-3337 | SCIENTISTS.UZ

Table 4. *Propagated uncertainties versus the resolution of the permittivity channel*

[redacted]	[redacted]	$5\cdot10^{-4}$	$2\cdot10^{-4}$	[redacted]	$5\cdot10^{-5}$	$2\cdot10^{-5}$
u(φ), %	0.656	0.164	0.066	0.033	0.016	0.007
u(ρ), kg/m³	21.43	5.36	2.14	1.07	0.54	0.21

Monte Carlo verification of the inversion

The Newton inversion was applied to noisy synthetic readings at three operating points, with 500 realizations each and a channel resolution of $1 \cdot 10^{-4}$. Table 5 reports the outcome. The standard deviations of the estimates agree with the propagated values in Table 4 to within 3%, which confirms that the linearized uncertainty analysis is adequate over this parameter range. The residual bias is two orders of magnitude smaller than the standard deviation and originates in the curvature of the mixture model rather than in the estimator.

Table 5. *Monte Carlo inversion results for 500 realizations per operating point*

φ, %	ρ, kg/m³	Bias in φ, %	Bias in ρ, kg/m³	SD of φ, %	SD of ρ, kg/m³
1.0	810	+0.0028	−0.098	0.0296	0.998
5.0	840	+0.0027	−0.089	0.0328	1.073
10.0	870	+0.0029	−0.092	0.0336	1.067

Tolerance to unknown water conductivity

The relaxation frequency depends on the conductivity of the water phase, which varies with salinity and is rarely known in service. The inversion was therefore run with the nominal value $1 \cdot 10^{-2}\ S/m$ while the synthetic data were generated with conductivities differing from it by up to a factor of three. Table 6 shows that the scheme is robust: a 50% error in the assumed conductivity displaces the density estimate by $0.11\ kg/m^3$ and the water fraction by 0.0034 %, both of which remain well within the noise-driven uncertainty. Only a threefold error produces a displacement comparable with the random component.

Table 6. *Effect of an incorrectly assumed water conductivity on the recovered parameters*

True σi, S/m	$5\cdot10^{-3}$	$8\cdot10^{-3}$	$1\cdot10^{-2}$	$1.5\cdot10^{-2}$	$3\cdot10^{-2}$
Error in φ, %	+0.0017	+0.0009	0.0000	−0.0034	−0.0217
Error in ρ, kg/m³	−0.057	−0.031	0.000	+0.113	+0.732

Discussion

The principal finding is qualitative before it is quantitative. The determinant of the Jacobian vanishes identically when the two frequencies coincide, so the second frequency is not an accuracy refinement but the condition that makes the estimation problem well-posed. This distinguishes the present treatment from the usual justification of multifrequency dielectric sensing, which appeals to improved discrimination without establishing that single-frequency operation is structurally incapable of the task. The locus in Table 2 makes the point concretely: the readings are not merely similar; they are identical.

The second finding concerns where the informativeness of the frequency axis originates. It does not originate from the mixture rule alone, because a non-dispersive mixture rule would give proportional responses at any two frequencies and a singular Jacobian. Interfacial polarization breaks the proportionality because the low-frequency limit depends on the host permittivity through a simple product with a function of φ, whereas the high-frequency limit couples the two parameters differently. This is why the observability map in Figure 4 is organized around f_{MW} rather than around any property of the electronics, and it explains why the design rule can be stated in units of f_{MW} rather than in hertz.

The third finding is a caution. The condition number of about $1\cdot10^{5}$ means that the problem, although observable, is ill-conditioned, and Figure 3 shows why: the two loci cross at a shallow angle because density modulates the hydrocarbon permittivity only within the narrow interval 2.030–2.173. Any claim of density measurement by this route must therefore be accompanied by a stated channel resolution.

ISSN: 2181-3337 | SCIENTISTS.UZ

Table 4 converts the requirement into a specification, and the specification is demanding: approximately 40 parts per million of the measured capacitance, maintained across the operating temperature range. That level is attainable only with active compensation of the transducer and links the present analysis to the broader design problem of the measurement channel rather than leaving it as an abstract result. The requirement therefore concerns not only instantaneous resolution but also resolution sustained over the verification interval, placing the result within the framework of metrological reliability rather than static accuracy (Sharipov et al., 2022).

The robustness to salinity deserves comment because it is not obvious in advance. One might expect the scheme to be fragile, since the relaxation frequency scales linearly with water conductivity and a salinity error therefore displaces the whole dispersion curve. The computations show otherwise because the design rule places both frequencies far from f_{MW}, in regions where the response has already saturated to its low- and high-frequency limits. Those limits are independent of conductivity. This robustness is therefore a consequence of the frequency-placement rule rather than an accident. It also indicates that operating close to f_{MW}, although it maximizes the dispersion slope, would be the wrong choice.

Several limitations should be stated. The Maxwell–Garnett rule assumes dilute, spherical, non-interacting inclusions; at volume fractions above roughly 0.15, the Hanai (1960) formulation or the integral modification of Qian et al. (2022) would be required, and the numerical values reported here would shift, although the observability argument would not. Droplet-size distribution and non-spherical shape introduce a distribution of relaxation times (Samet et al., 2022; Sillars, 1937), which broadens the transition and reduces the effective dispersion depth. Temperature has been held constant throughout; in service, it acts on both phases and constitutes a third parameter, so a three-parameter observability analysis with an independent temperature reading is the natural continuation of this work. Finally, all results presented here are model-based; experimental confirmation using prepared emulsions of known composition remains to be carried out.

Conclusions and Implications

Water content and hydrocarbon density cannot be separated from a single capacitive reading: the Jacobian of the measurement map is singular at any one frequency, and an entire locus of composition–density pairs produces the same permittivity. Maxwell–Wagner interfacial polarization removes the degeneracy; therefore, a two-frequency scheme is a necessary condition for observability rather than an optional improvement.

Three results are of direct use in instrument design. The frequencies should be placed at or below $0.05 \cdot f_{\mathrm{MW}}$ and at or above $10 \cdot f_{\mathrm{MW}}$; beyond this separation the gain saturates within 1%, so extreme frequencies are unnecessary. The channel resolution required to make density meaningful is $1 \cdot 10^{-4}$ in relative permittivity, giving standard uncertainties of 0.033% in water volume fraction and 1.07 kg/m³ in density, values confirmed by Monte Carlo inversion. The scheme tolerates a 50% error in the assumed water conductivity with a density displacement of only 0.11 kg/m³, because the recommended frequencies lie in the conductivity-independent limits of the response.

The resolution requirement is the practical bottleneck and defines the next stage of the work: a capacitive channel with periodic autocalibration against an internal standard and adaptive compensation of influencing quantities, without which the two-frequency scheme remains observable in principle but unusable in practice. Experimental validation using emulsions of certified composition and extension of the observability analysis to include temperature as a third parameter are the two further steps required before the method can be offered for metrological attestation.

REFERENCES

1. Adohi, B. J. P., Vanga Bouanga, C., Fatyeyeva, K., & Tabellout, M. (2009). Application of the Maxwell–Wagner–Hanai effective medium theory to the analysis of the interfacial polarization

ISSN: 2181-3337 | SCIENTISTS.UZ

relaxations in conducting composite films. *Journal of Physics D: Applied Physics, 42*(1), 015302. https://doi.org/10.1088/0022-3727/42/1/015302

2. Asami, K. (2002). Characterization of heterogeneous systems by dielectric spectroscopy. *Progress in Polymer Science, 27*(8), 1617–1659. https://doi.org/10.1016/S0079-6700(02)00015-1
3. Böttcher, C. J. F. (1973). *Theory of electric polarization* (2nd ed., Vol. 1). Elsevier.
4. Hanai, T. (1960). Theory of the dielectric dispersion due to the interfacial polarization and its application to emulsions. *Kolloid-Zeitschrift, 171*(1), 23–31. https://doi.org/10.1007/BF01520320
5. Joint Committee for Guides in Metrology. (2008). *Evaluation of measurement data—Guide to the expression of uncertainty in measurement (JCGM 100:2008)*. https://doi.org/10.59161/JCGM100-2008E
6. Jumamuratov, B. A., Abduqayumov, A. A., & Eshmuradov, D. E. (2024). Kompozit materiallarning radioshofonligini nazorat qiluvchi vositaning metrologik ta'minoti [Metrological support for a means of controlling the radio transparency of composite materials]. *Milliy Standart*, (3), 1–5.
7. Kaatze, U. (1989). Complex permittivity of water as a function of frequency and temperature. *Journal of Chemical & Engineering Data, 34*(4), 371–374. https://doi.org/10.1021/je00058a001
8. Kalman, R. E. (1963). Mathematical description of linear dynamical systems. *Journal of the Society for Industrial and Applied Mathematics, Series A: Control, 1*(2), 152–192. https://doi.org/10.1137/0301010
9. Maxwell, J. C. (1873). *A treatise on electricity and magnetism* (Vol. 1). Clarendon Press.
10. Qian, J., Yan, S., Li, Z., Yu, L., Wang, X., Zhang, Z., Sun, J., & Han, X. (2022). Modification of the Maxwell–Wagner heterogeneous dielectric model for heterogeneous polymers and emulsions. *Polymers, 14*(13), 2743. https://doi.org/10.3390/polym14132743
11. Samet, M., Kallel, A., & Serghei, A. (2022). Maxwell–Wagner–Sillars interfacial polarization in dielectric spectra of composite materials: Scaling laws and applications. *Journal of Composite Materials, 56*(20), 3197–3217. https://doi.org/10.1177/00219983221090629
12. Sharipov, G. N., Turayeva, N. M., & Eshmuradov, D. E. (2022). Voprosy povysheniya metrologicheskoy nadezhnosti sredstv izmereniy [Issues in improving the metrological reliability of measuring instruments]. In *Proceedings of the International Conference "State and Trends in the Development of Standardization and Technical Regulation in the World"* (pp. 178–184). Tashkent State Technical University.
13. Sihvola, A. (1999). *Electromagnetic mixing formulas and applications*. Institution of Electrical Engineers.
14. Sillars, R. W. (1937). The properties of a dielectric containing semiconducting particles of various shapes. *Journal of the Institution of Electrical Engineers, 80*(484), 378–394. https://doi.org/10.1049/jiee-1.1937.0058
15. Wagner, K. W. (1914). Erklärung der dielektrischen Nachwirkungsvorgänge auf Grund Maxwellscher Vorstellungen. *Archiv für Elektrotechnik, 2*(9), 371–387. https://doi.org/10.1007/BF01657322